Nodular Structure of Isotactic Polypropylene Crystallizes from the Melt

Yousef A. Mubarak

Chemical Engineering Department, Faculty of Engineering and Technology, University of Jordan, Amman 11942, Jordan

ABSTRACT: This article highlights the melt crystallization behavior of different grades of isotactic polypropylene (iPP) using a hot-stage polarizing optical microscopy. iPP samples were heated up at a heating rate of 10°C/min passing the melting temperature and then kept for 3 min at a temperature range of 175–200°C before they cooled rapidly at 40°C/min to crystallize isothermally at a range of 130–145°C. It has been found that the temperature at which the samples were kept has a strong effect on the crystallization mode; for samples heated up and kept at temperatures below 190°C, the crystallization started with thin and long rods or nodules, which grew in the circumferential direction only while their lengths remain unchanged as the time passed. The shape of the nodules can be straight, circular, branched, or entangled, and they can grow parallel to each other or they can be crossed or in a random way. This phenomenon disappeared completely for samples melted and kept at temperatures above 195°C. © 2011 Wiley Periodicals, Inc. J Appl Polym Sci 122: 2228–2243, 2011

Key words: isotactic polypropylene; morphology; crystallization; nodular

INTRODUCTION

Isotactic polypropylene (iPP) can crystallize into monoclinic α-structure, hexagonal β-structure, triclinic γ-structure, and a mesomorphic structure.[1–4] Formation of different polymorphic forms can be controlled by the conditions of crystallization and/or by the addition of special nucleating agents. Formation of monoclinic α-structure can be achieved by a slow cooling of the quiescent melt, whereas the presence of special nucleating agents or crystallization at high pressure produces hexagonal β-structure or triclinic γ-structure, respectively. On the other hand, the mesomorphic structure, which is intermediate between amorphous and crystal forms of iPP, can be obtained either by rapid melt-crystallization or by crystallization from the glassy state.[5–7] Polymorphs of α, β, and γ are related to the typical lamellar crystal morphology, whereas the characteristic feature of the mesomorphic form of iPP is the formation of nonlamellar domains. The structure and morphology of iPP obtained as a function of the conditions of crystallization can be further modified by annealing.[8,9] By varying the conditions of crystallization, a range of crystal structures and morphologies of iPP can be obtained, which in turn allows controlling the properties in a wide range.

The structure and morphology of quench-induced mesophase have been widely studied. Early electron microscopic studies by Gezovich and Geil[10] revealed the nodular (granular) structure in quenched i-PP film, and they suggested that there was "granular-like" structure, which had small and imperfect hexagonal crystallites in the film. Ogawa et al.[11] studied the size distribution of nodules on the surface of polypropylene (PP) films crystallized from the glass and subsequently annealed. The authors reported that the origin of the nodule was the crystallite produced by the growth of many nuclei, which were generated on crystallization from the glass and survived on annealing. The surviving nuclei grow until they collide with the neighbors.

An ultraquenching technique is used by Hsu et al.[5] to prepare glassy isotactic PP films of thickness up to 0.3 mm. The structure and properties of the as-quenched and subsequently crystallized samples were characterized by various techniques. X-ray diffraction shows PP crystallizes from the glass into a smectic structure at −20°C and then transforms to monoclinic microcrystals at 40°C; a nodular structure was observed on the surface. Annealing above the α-relaxation temperature results in an increase in the nodule size. The authors found that the transformation temperature increases with the film thickness. A study is presented by Norton and Keller[12] in which

the authors crystallized a range of commercial iPP-s in the temperature range 100–150°C. The investigation has centered on the five different spherulite types, as identified optically, which were then correlated with the details of their particular lamellar morphology. It was found that each spherulite type is characterized by virtue of the arrangement of its constituent lamellae, in terms of orientation, habit type, and crystal structure. Thus, specific correlations were obtained between the structural entities on all scales of the structure hierarchy. Caldas et al.[13] used a scanning transmission electron microscopy to study the amorphous matrix of quench-cooled iPP. The dark field images revealed the existence of microcrystalline regions, 10–20 nm in size, that have the α-monoclinic crystal form. Regions of lower crystalline order are also observed, which, according to micro–micro diffraction, also possess the α-monoclinic crystal structure but with substantially larger unit cell constants. Differential scanning calorimetry studies by the same authors indicate that during quench cooling to the glassy state iPP samples attain a low degree of crystalline order, and upon heating from the glassy state, these samples exhibit exothermic transitions, between −15 and 120°C, that correspond to the formation and subsequent perfection of the microcrystalline regions.

A gradual deformation at the fiber surface from a spherulitic structure to a shish–kebab-type structure is observed using a scanning probe microscopy when the investigation of changes in the morphology of PP monofilaments during melt-extrusion and subsequent drawing is studied by Risnes et al.[14] The effect of nucleating agent on the crystalline morphology under different structure levels of PP materials was investigated by Xu et al.[15] The authors reported that increasing nucleating agent has an effect on both high and low levels of the crystalline structure, the nucleating agent displayed a heterogeneous nucleation effect. It is also reported that it is more stable for PP crystallization from a melt to form a gyroidal structure, with random coil molecules first transforming to the gyroidal structure as quickly as possible. Konishi et al.[16] studied the crystallization process of iPP by heating from the prequenched mesomorphic phase. The authors mentioned that mesomorphic iPP as quenched shows the well-known nodular structure, and during the heating process, the nodules grew larger maintaining self-similarity, with the mesomorphic phase partially transforming into the crystalline phase inside the nodules.

Zia et al.[17] used a controlled rapid cooling technique to melt-crystallize iPP at different cooling rates and subsequently annealed it at an elevated temperature. Mesomorphic domains were obtained by fast cooling from the melt at a rate larger than about 95°C/s. These domains stabilize upon heating by growing in chain direction and cross-chain direction. Formation of different types of lamellae was reported when the samples annealed at 160°C. It is suggested by the authors that these lamellae either develop by coalescence of nodules or by recrystallization from the melt. The transition from the disordered mesomorphic structure to monoclinic structure on heating at about 340 K occurs at a local scale within existing crystals and cannot be linked to complete melting of mesomorphic domains and recrystallization of the melt. Quenched mesomorphic iPP precursor material has been investigated by Zaho et al.[18] as well as the material annealed at different temperatures. It is reported that the nodular morphology of the mesomorphic remains constant for annealing temperatures T_a below 120°C, while needle-like or leaf-like crystals form when T_a approaches the melting temperature.

It is very obvious from the presented literature above that PP is one of the most studied polymers, its structure and properties are well documented, but despite all these efforts, important questions regarding crystallization are not completely answered. To the best of our knowledge, this is the first visualization of iPP crystallizes into rod or nodular shape directly from the molten phase without the formation of mesomorphic structure or recrystallization from the glassy state and then followed by annealing.

EXPERIMENTAL

Materials

Five virgin iPP homopolymer samples were used: (1) grade 578P provided by Sabic Co. KSA which has a melt flow index (MFI) of 11 g/10 min; (2) grade HP525J produced by Moplen and has a density of 900 kg/m^3 and a melt flow index of 2.8 g/10 min; (3) grade M3661 made via TOTAL and has a melt flow index of 14 g/10 min; (4) total PPH5042 PP with 6 g/10 min melt flow index and a density of 905 kg/m^3; (5) FINA nucleated iPP 4042S with melt flow rate of 3 g/10 min.

Another three samples were prepared and used as well where Moplen HP525J is mixed with 1 wt % of nanofil 9 in the first, mixed with 5 wt % polyether block amide (PBA) in the second, and in the third Moplen HP525J is mixed with 10 wt % of PBA. Nanofil 9 used in this study is produced by Rockwood Additives and is used as obtained from the producer. It consists of organically modified nanometer scale, layered magnesium aluminum silicate platelets. The silicate platelets that Nanofil 9 is derived from are 1 nm thick and 70–150 nm across. These platelets are surface modified with an organic chemistry to allow complete dispersion into and provide miscibility with the thermoplastic systems for
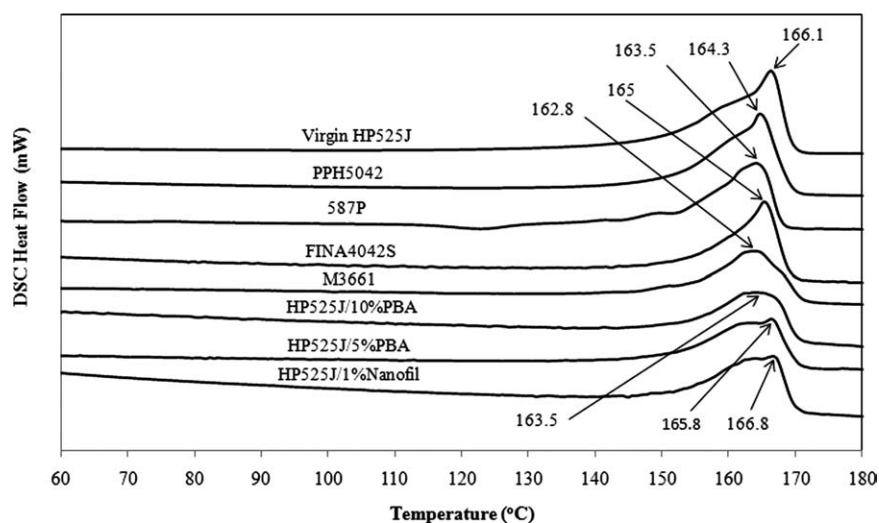
Figure 1 DSC heat flow curves for iPP samples used in the present study, and the samples were nonisothermally crystallized (10°C/min) from a temperature of 200°C.

which they were designed to improve. Nanofil 9 is crème in color and has a density of 1800 kg/m³ and average particle size of 8 μm. PBA produced by Arkema has a density of 1010 kg/m³ and a melt flow index of 7 g/10 min.

Composites preparation

The three composites used in this study were prepared as follows: the blends were prepared by melt-compounding on a Brabender PL2100 Plasticorder with a batch-type roller mixer, the average weight of each batch was 40 g. The compounding was done at a temperature of 210°C for 8 min and at a rotor speed of 60 rpm. On completion of the blending step, the sample was taken out from the bowl of the brabender

and naturally cooled to room temperature before it is chopped to small pieces using a mill machine equipped by a steel blade to reduce the size of the particles. Strips with dimensions of 25 × 1 mm were produced from the chopped blends using a Brabender PL2100 single screw extruder, the temperature distribution throughout the extruder was 167, 185, 200, and 220°C from the hopper side to the die side with a speed of 30 rpm for the screw, and the chiller temperature was set at 50°C. These strips were used in the thermal and morphological study.

Differential scanning calorimetry

Differential scanning calorimetry (DSC) experiments were performed using a power-compensation-based
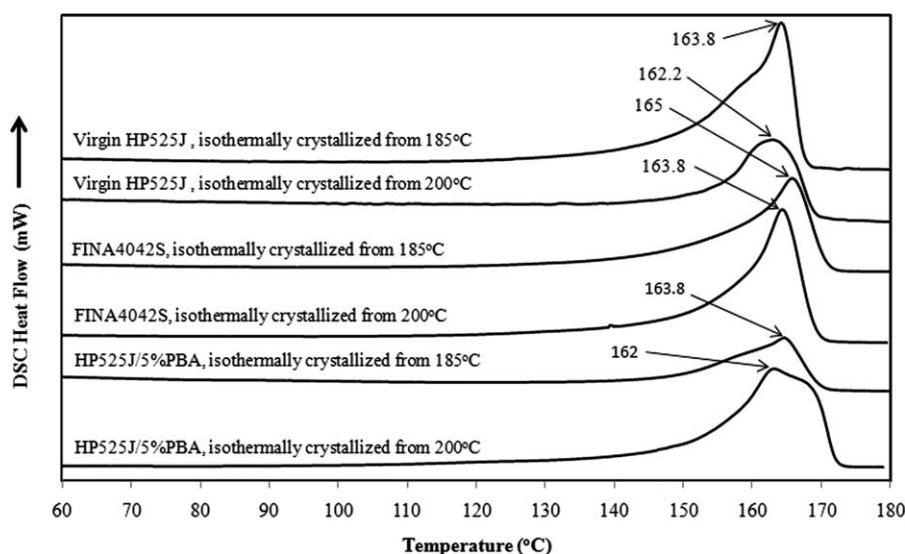

Figure 2 DSC heat flow curves for iPP samples used in the present study, and the samples were isothermally crystallized (135°C/min) from a temperature of 200 and 185°C.
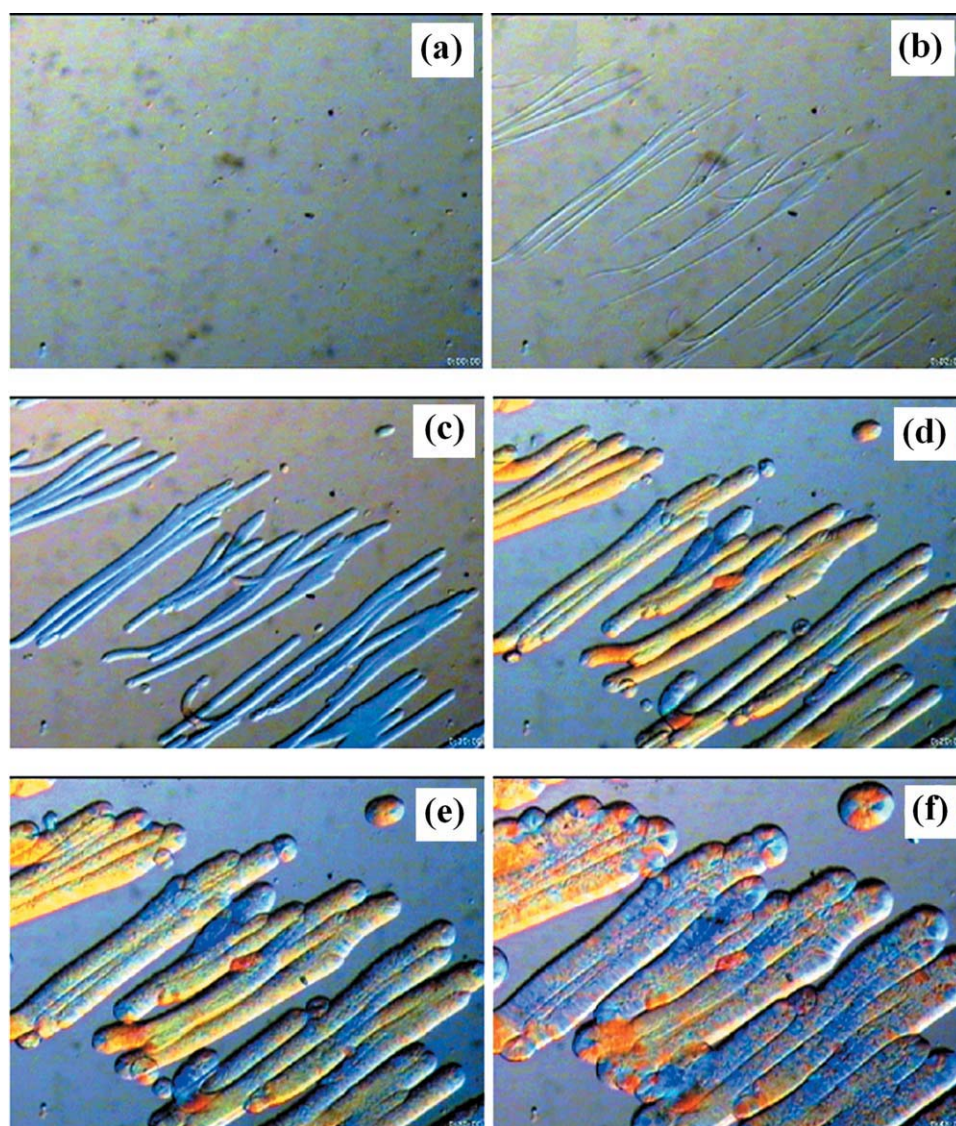
Figure 3 Images of iPP (Grade HP525J) isothermally crystallized at 140°C. The melt temperature was 185°C (magnification = 190×). (a) The molten sample at 185°C; (b) the sample after about 1.5 min at an isothermal crystallization at 140°C; (c) the same sample after 4 min; (d) after 10 min; (e) after 20 min; (f) after 30 min. [Color figure can be viewed in the online issue, which is available at wileyonlinelibrary.com.]

differential scanning calorimeter DSC-7 (Perkin–Elmer). The instrument was operated in conjunction with the cryogenic cooling accessory CCA-7, ensuring a constant temperature of the heat sink. The sample and reference furnaces were purged with nitrogen gas at a flow rate of 40 mL/min. Calibration of the sensor temperature and of the heat-flow rate was done according to standard procedures, using indium and tin as calibrants. Circular and flat samples with a mass of about 5 mg were cut from the PP resin or produced strips and placed in the aluminum pans (Mettler-Toledo).

Samples were first heated from 25 to 200°C at a rate of 10°C/min and kept at this temperature for 3 min to eliminate any thermal history. For isothermal crystallization, iPP samples were rapidly cooled to 135°C and kept at this temperature to crystallize while for nonisothermal crystallization the iPP samples were cooled at a rate of 10°C/min to the room temperature. A second heat scan at 10°C/min was then carried out from 25 to 200°C to obtain the final sample enthalpy of fusion curve from which melting temperatures of used samples and type of crystals formed were obtained. To check if there is any effect for the initial temperature from which the molten polymer is cooled down, different samples were heated at a heating rate of 10°C/min from 25 to 185°C before they were cooled down rapidly to 135°C and left to crystallize isothermally. Again, a second heat scan at 10°C/min was then carried out
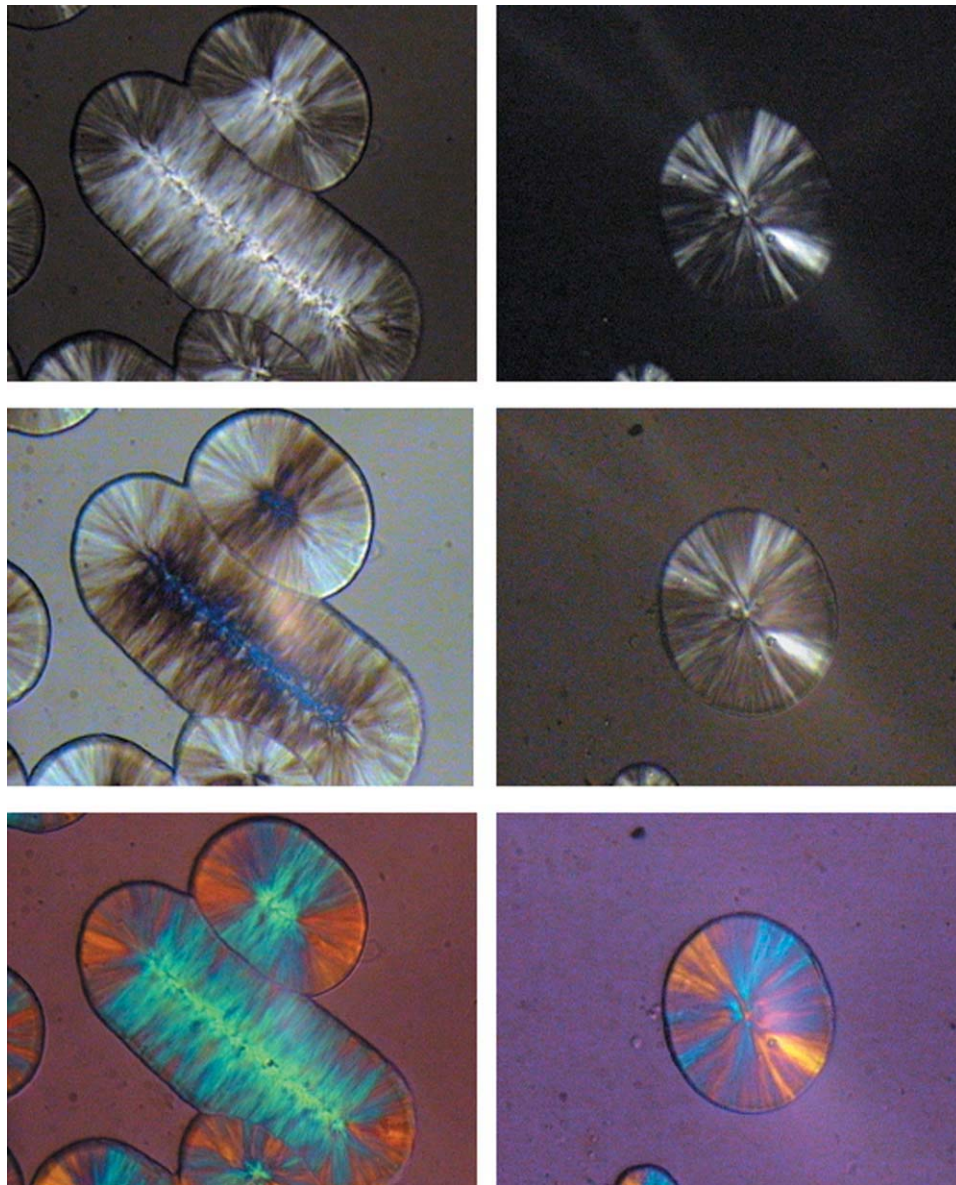
Figure 4 IPP (Grade HP525J) isothermally crystallized at 135°C from a melt temperature of 185°C showing the mixed birefringence α-structure of individual spherulite (right) and nodules (left) (magnification = 780×). [Color figure can be viewed in the online issue, which is available at wileyonlinelibrary.com.]

from 25 to 200°C to obtain the final sample enthalpy of fusion curve from which the type of crystals formed can be detected.

Polarized light microscopy

Information about the structure of melt-crystallized samples was gained by polarizing optical microscopy, using a ML9430-Meiji Techno-Japan microscope equipped with a (Mettler FB82-USA) hot stage and a Sony digital camera. PP samples were cut from the virgin PP resin or from the produced composite strips and then sandwiched between two microscope cover glasses. Samples were first melted at a heating rate of 10°C/min, pressed into thin film, and then kept for 3 min at different temperatures (175, 180, 185, 190, and 200°C). On termination of the 3 min period of time, the molten samples were cooled rapidly to the required crystallization temperature at a rate of 40°C/min, and the temperature was maintained during the period of time required to complete the crystallization process. A Sony digital camera fixed on top of the microscope tube and connected to the PC by a TV card and a video recorder software were used to record the crystallization process and then take and store the images. Several samples were tested twice or three times to ascertain the reproducibility of the results.
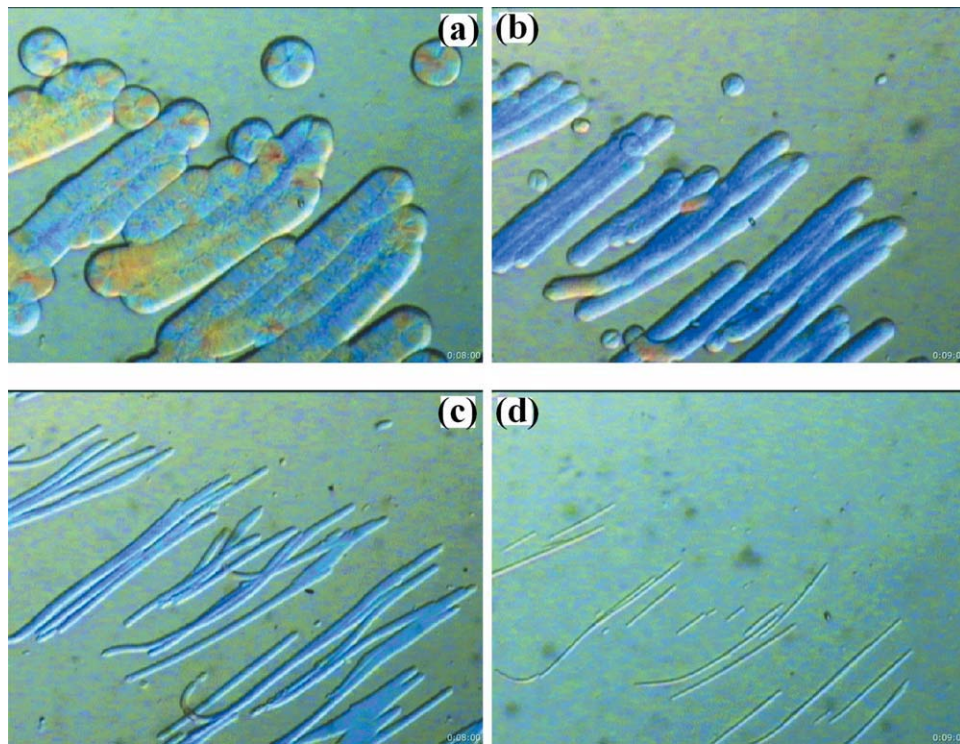
Figure 5 Images of iPP (Grade HP525J) isothermally crystallized from the melt at a crystallization temperature of (a) 130; (b) 135; (c) 140; (d) 145°C (magnification = 190×). [Color figure can be viewed in the online issue, which is available at wileyonlinelibrary.com.]
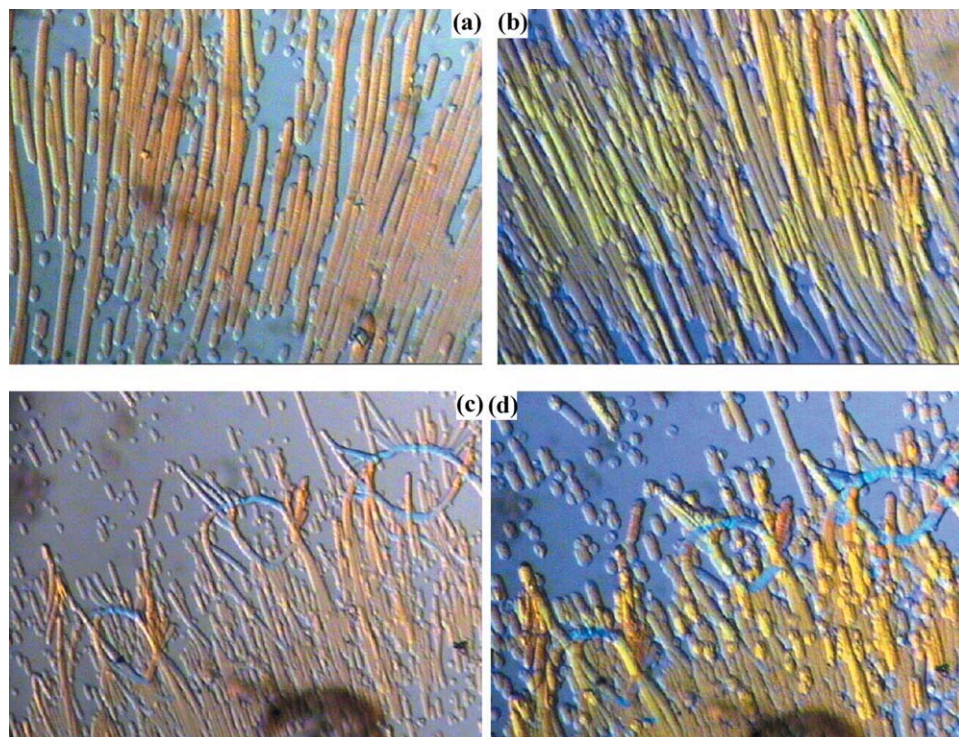

Figure 6 IPP HP525J isothermally crystallized at 135°C. The melt temperature was 175°C (magnification = 190×). [Color figure can be viewed in the online issue, which is available at wileyonlinelibrary.com.]
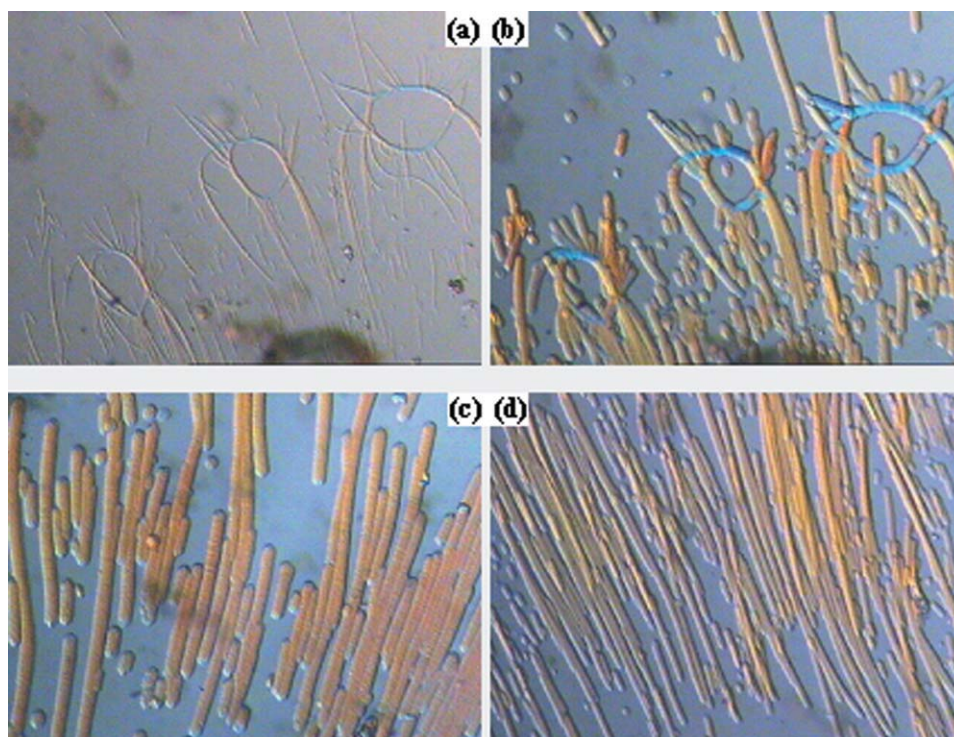
Figure 7 IPP HP525J isothermally crystallized at 135°C. The melt temperature was 180°C (magnification = 190×). [Color figure can be viewed in the online issue, which is available at wileyonlinelibrary.com.]

RESULTS AND DISCUSSION

Melting temperature and crystals type

Figure 1 displays the DSC heat flow curves for the samples used in this study. It is clearly seen that the melting temperatures ranged from 162.8 to 166.8°C. Although there are little changes between the obtained melting temperatures for the samples used, the curves reveal only one type of crystals, which is the monoclinic α-structure, with no evidence of any presence of the hexagonal β-structure, which has a melting temperature of $T_m = 146°C^{19}$ or triclinic γ-structure.

The effect of the molten iPP temperature from which the cooling step started to crystallize the samples isothermally is presented graphically in Figure 2. The DSC heat scans prove that only the monoclinic α-structure is present within the obtained structure regardless the temperature of the iPP from which the cooling stage is started. The figure shows that there is a little variation in the melting temperature of the crystallized samples. It seems that the presence of the nodular structure with its close packing of the crystals results in an increase in the melting temperature, this phenomenon was observed actually using the PLM, where during the melting step for samples containing nodular structure, it is observed that the spherulites melted before the nodules.

Melt crystallization into nodular structure

Figure 3 shows a set of images of iPP grade HP525J isothermally crystallized from the molten state. Initially, the sample's temperature was raised up to 185°C passing through the melting temperature (T_m = 166.1) and kept at this temperature for a period of 3 min. Then, the temperature was decreased down to 140°C at a cooling rate of 40°C/min and then kept at this temperature until crystallization is completed. Figure 3(a) shows the molten sample at 185°C, it is clearly seen that only a molten phase without any appearance of any crystal is presented. Once the temperature was reduced to 140°C, thin and long nodules or rods appeared after about 1.5 min as shown in Figure 3(b). As the crystallization continued, the nodules grew in the circumferential direction and became thicker while their length remained unchanged as clearly seen in Figure 3(c–f); the nodules circumferential growth continued until they impinge with each other or with other spherulites.

In addition to the nodules, Figure 3 shows some individual spherulites growing within the sample at the same time. The coexisting of individual spherulites and nodules are the result of two different crystallization events during cooling from the melt. The formation of qualitatively different crystal morphologies by the variation of the rate of melt-crystallization
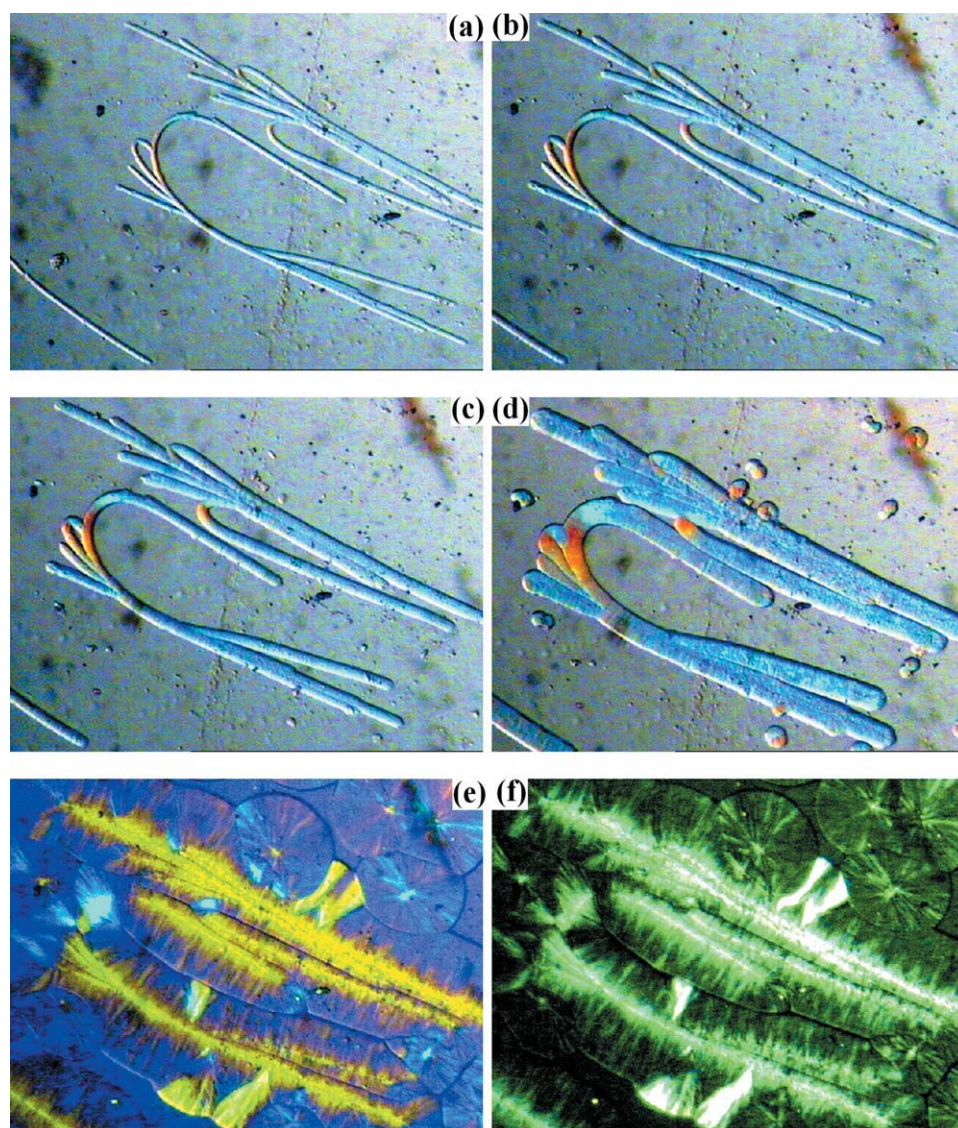
Figure 8 IPP HP525J isothermally crystallized at 135°C. The melt temperature was 185°C (magnification = 190×). [Color figure can be viewed in the online issue, which is available at wileyonlinelibrary.com.]

was also observed in a 100-nm thick film of PVDF. Melt-crystallization in air produced lamellar crystals and spherulites.[20] In contrast, replacing of the cooling medium with ice-water or liquid nitrogen produced nodules of size of about 20–30 nm. The coexistence of both nodules and lamellae was detected on quenching in water kept at room temperature, an increase of the size of nodules as well as the thickness of lamellae was observed, if the temperature of the cooling medium, that is, water, was increased.[21] Zaho et al.[18] found that during the annealing process for quenched mesomorphic iPP, only the crystalline ordering increases during the transition, but not the size of the nodules. Also reported is that after the transition the geometry of the nodules changes considerably, whereas there is little additional increase of crystalline ordering.

Additionally, Hsu et al.[5] found that annealing of glassy iPP films obtained by an ultraquenching technique above the α-relaxation temperature results in an increase in nodule size. The size distribution of nodules on the surface of PP films crystallized from the glass and subsequently annealed was studied by Ogawa et al.[11] The author reported that the origin of the nodule was the crystallite produced by the growth of many nuclei, which were generated on crystallization from the glass and survived on annealing; the surviving nuclei grow until they collide with the neighbors.

It is noticed that during the growth of an individual spherulite, a mixed (negative/positive) birefringence is obtained. It was very difficult to observe the exact birefringence when a nodular structure is monitored; the spherulites were growing attached to
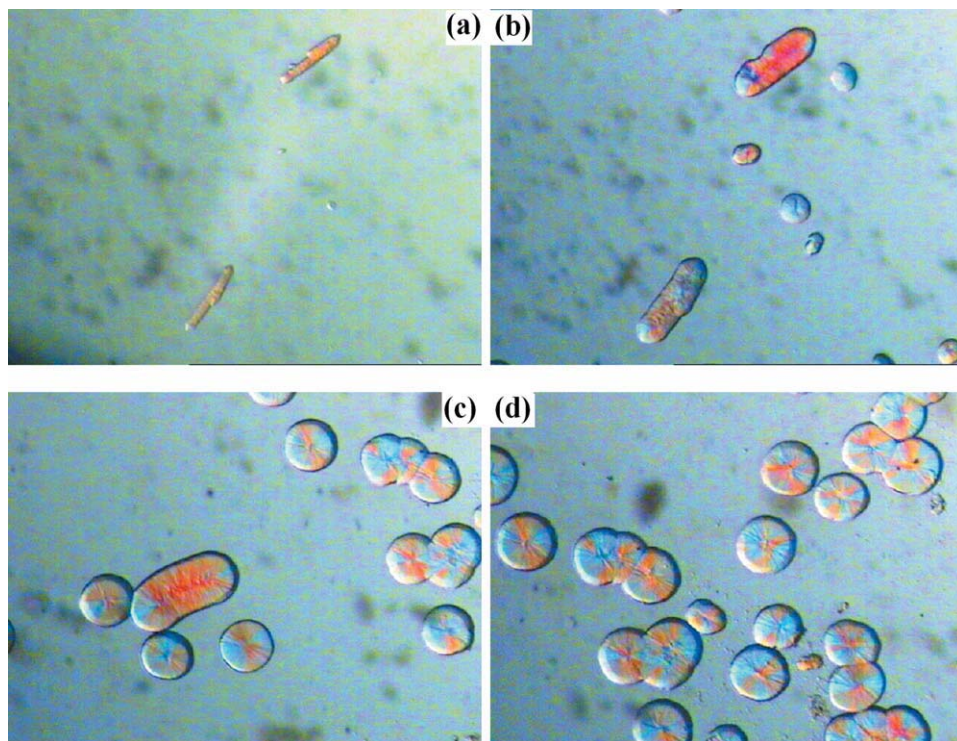
Figure 9 IPP HP525J isothermally crystallized at 135°C. The melt temperature was 190°C (magnification = 190×). [Color figure can be viewed in the online issue, which is available at wileyonlinelibrary.com.]

each other in the same rodlike, which makes it very difficult to distinguish the birefringence, but there were no appearance of β or γ structures within the nodules. The obtained nodular structure is almost close to the mixed birefringence α-spherulite as shown in Figure 4.
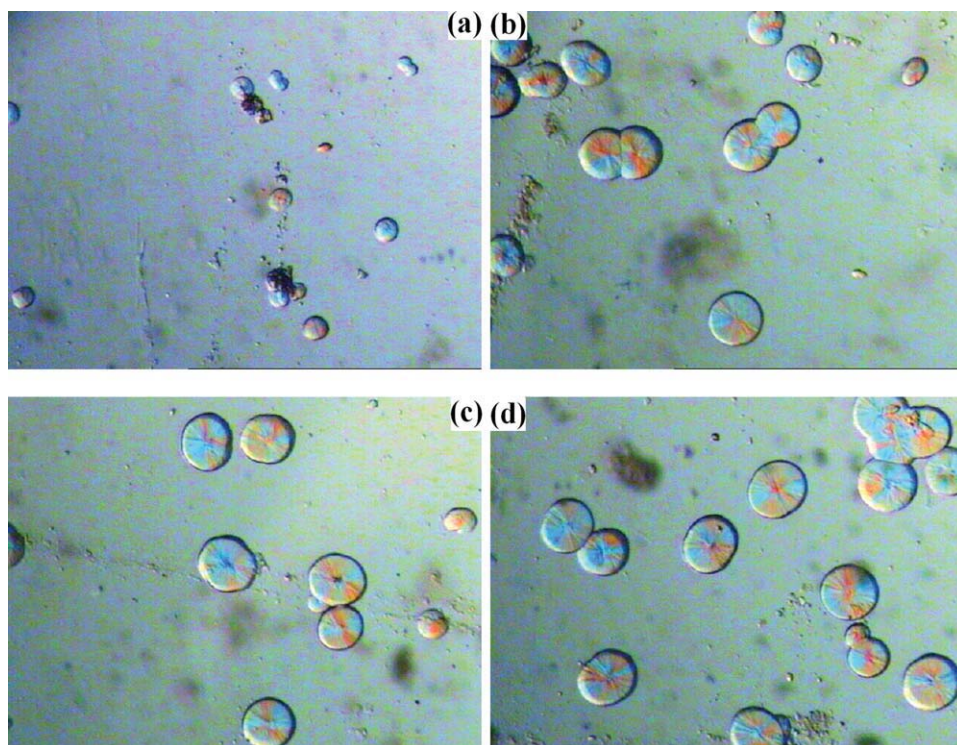

Figure 10 IPP HP525J isothermally crystallized at 135°C. The melt temperature was 200°C (magnification = 190×). [Color figure can be viewed in the online issue, which is available at wileyonlinelibrary.com.]
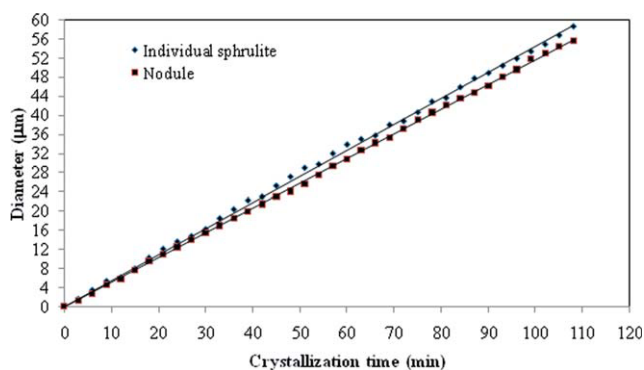
Figure 11 Growth rates of individual monoclinic α-spherulites and nodules isothermally crystallized at 145°C from an iPP HP525J melt at a temperature of 185°C. Both the spherulites and nodules were growing together within the same melt. [Color figure can be viewed in the online issue, which is available at wileyonlinelibrary.com.]
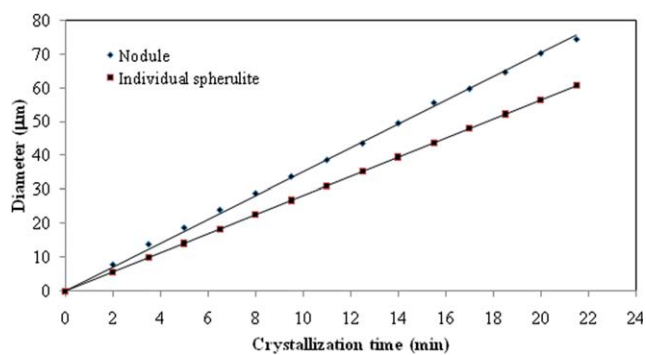
Figure 12 Growth rates of individual monoclinic α-spherulites and nodules isothermally crystallized in different samples at 135°C from an iPP HP525J melt. Melt temperature was 200 for the spherulites while the melt temperature was 185°C for the nodules. [Color figure can be viewed in the online issue, which is available at wileyonlinelibrary.com.]
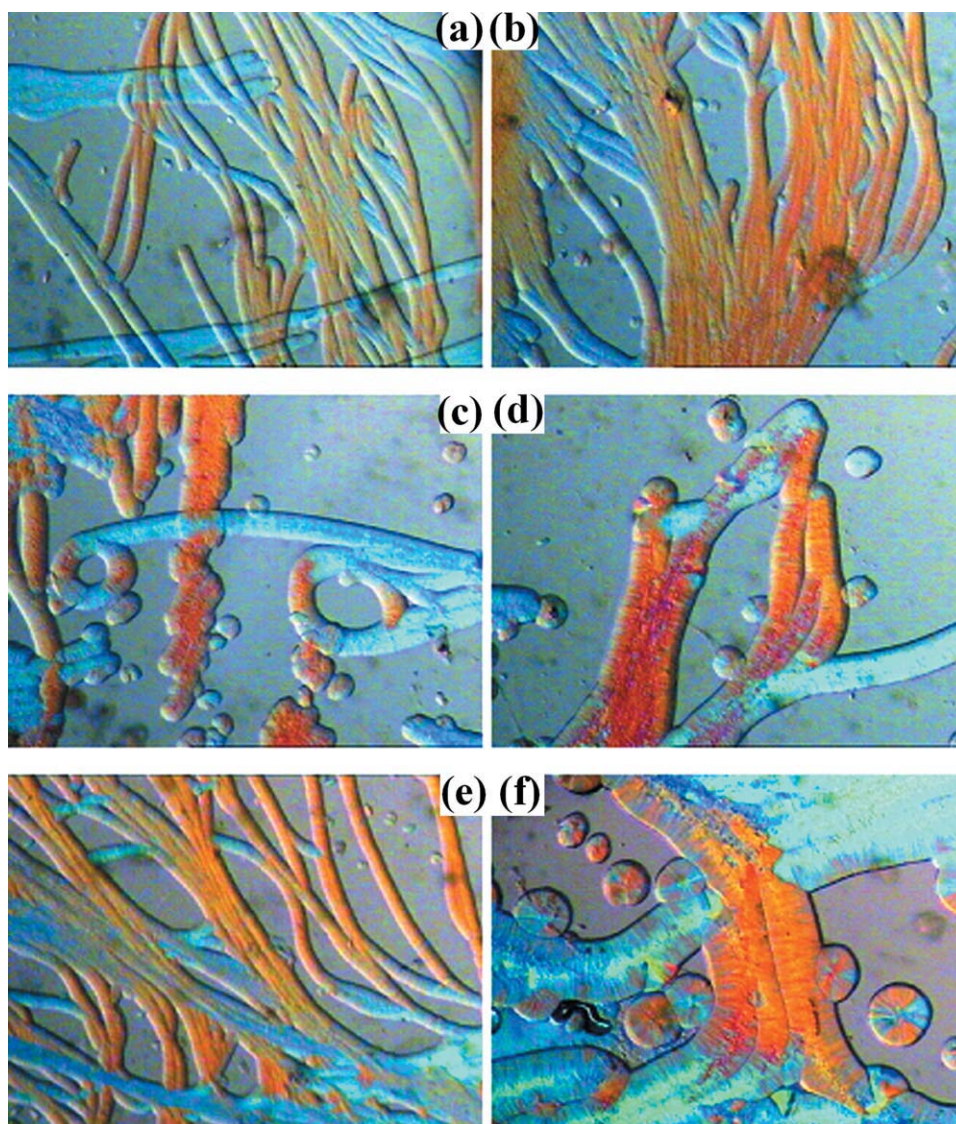

Figure 13 Images of iPP (Total M3661) isothermally crystallized at 135°C. The melt temperature was 185°C (magnification = 190×). [Color figure can be viewed in the online issue, which is available at wileyonlinelibrary.com.]

Figure 14 Images of iPP (HP525 mixed with 10 wt % PBA) isothermally crystallized at 135°C. The melt temperature was 185°C (magnification = 190×). [Color figure can be viewed in the online issue, which is available at wileyonlinelibrary.com.]
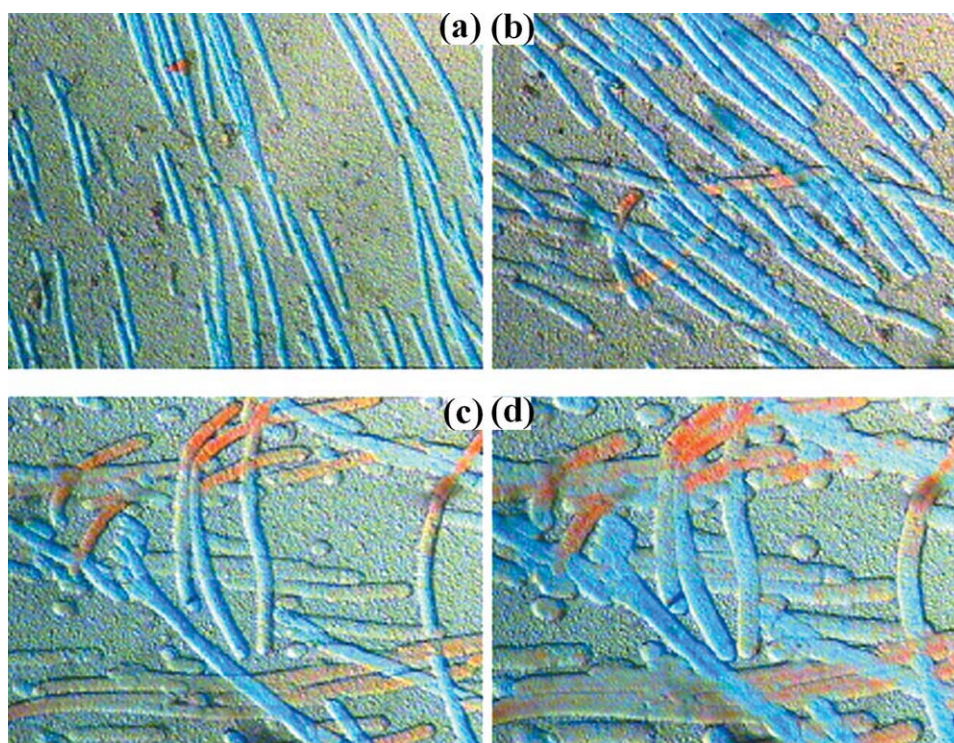
Effect of isothermal crystallization temperature

A set of images for iPP samples isothermally crystallized from the melt at different temperatures are presented in Figure 5, with images taken after 8 min of the crystallization step. All samples were heated up to a temperature of 185°C before they cooled rapidly to the required crystallization temperature. A theoretical interpretation for the size reduction of the nodules diameter with increasing the crystallization temperature was given by Wunderlich[22] who states that the thermodynamic barrier of growth is linear with ΔT^{-1}, where ΔT is the difference between the melting and crystallization temperatures. So, increasing the crystallization temperature will reduce ΔT, reducing ΔT will increase ΔT^{-1} and hence increase the thermodynamic barrier.

Effect of melt's temperature

The set of figures from Fig. 6–10 show the melt crystallization of iPP grade HP525J samples isothermally crystallized at 135°C as a function of molten phase's temperature. The images reveal that the intensity of the crystallized nodules decreases as the temperature of the molten phase increases. The intensity of the nodules for samples heated up to a temperature of 175°C (10° above the melting temperature of the monoclinic α-crystals) is much higher than the intensity of the same samples heated up to a temperature of 190°C before they cooled rapidly to 135°C to isothermally crystallize. Nodular structure disappeared completely for samples crystallized from melting temperature of 200°C as clearly show in Figure 10.

To erase any previous morphological or heat history of iPP, the samples should be heated up to a temperature above 190°C and maintained at this temperature for a short period of time; otherwise, the morphological history will remain within the samples.[23,24] In the present work, it is found that heating iPP samples up to a temperature exceeding the melting temperature by about 25–30°C will not remove the morphological history of the samples. Within this melting temperatures range, crystallization of such samples will produce nodules with different intensities; these nodules grow only in the circumferential direction until they impinge with another growing nodule [Fig. 8(e,f)] or neighbor crystals. As the temperature of iPP sample approaches 190°C, only a little number of nodules crystallizes (Fig. 9) while the number of individual crystals will increase. Figure 9 shows melt crystallization of iPP sample heated up to a temperature 200°C before isothermal crystallization carried out at 135°C; it is clearly seen that only individual
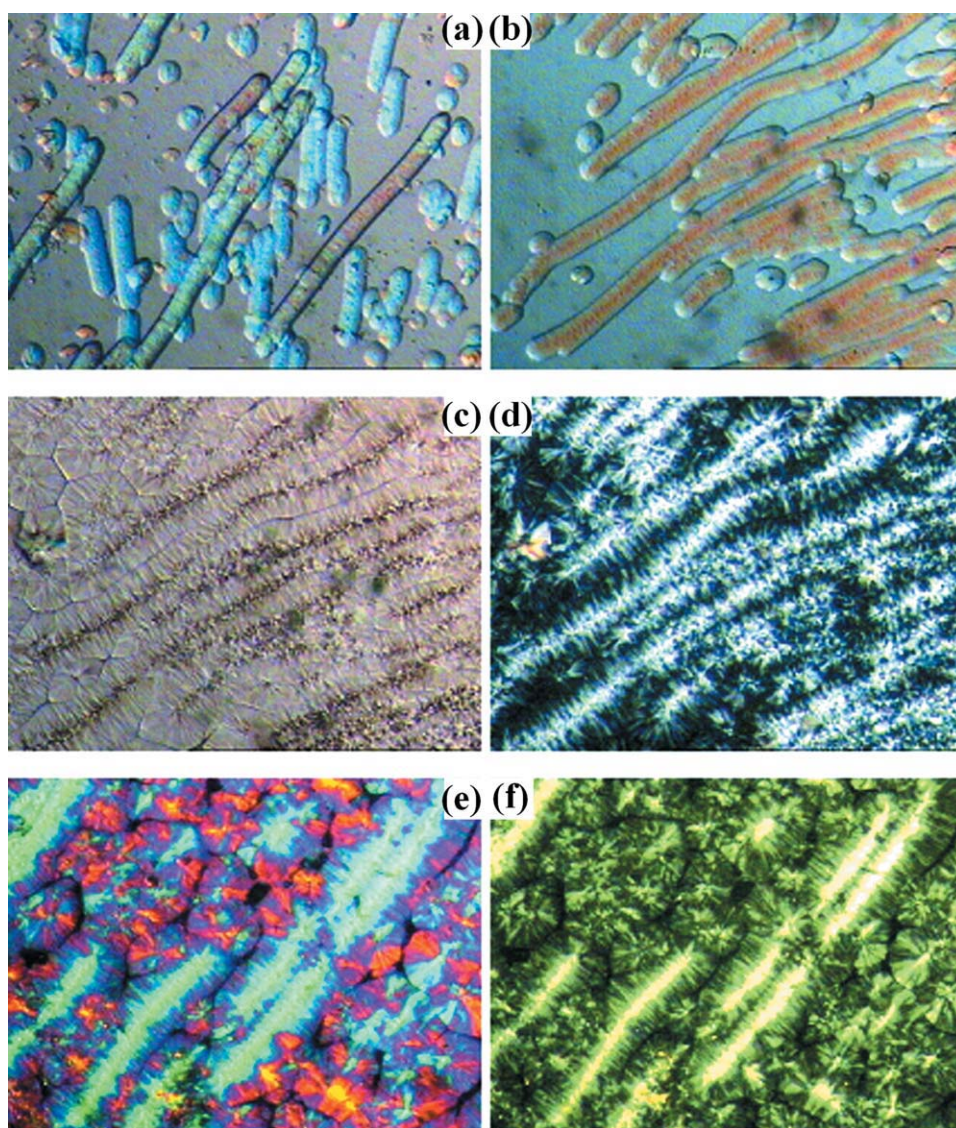
Figure 15 Images of iPP (HP525 mixed with 5 wt % PBA) isothermally crystallized at 135°C. The melt temperature was 185°C (magnification = 190×). [Color figure can be viewed in the online issue, which is available at wileyonlinelibrary.com.]

monoclinic α-spherulites are crystallized, and nodules disappear completely throughout the sample.

Growth rate of nodules

In an attempt to compare growth rates of individual monoclinic α-spherulites and nodules both crystallized from the melt and within the same sample, individual spherulite and nodule diameters were measured as a function of time and presented in Figure 11. The slope of the straight line of the diameter against the time gives the growth rate (G), $G = \frac{dr}{dt}$. The isothermal growth rate of the individual iPP spherulite at 145°C is constant and equals to 0.545 μm/min, and constant isothermal growth rates for iPP is reported in the literature.[25,26] Also, the circumferential growth of the nodule is found to be

constant, where $G = 0.516$ μm/min. It is clearly seen that there is not much difference between the two growth rates slopes, but individual spherulite grows a little faster than the nodule. It seems that the attachment of the spherulites within the same nodule reduces the growth rate compared to the growth rate of individual spherulites.

A comparison between growth rates for individual spherulite growing in a sample heated up to 200°C with a nodule growing in a sample heated up to 185°C is presented in Figure 12. Both samples were isothermally crystallized from the melt at 135°C. The results showed that growth rates of nodules are greater than those for individual spherulite grown at similar condition, with the growth rate for the individual spherulite found to be 2.81 μm/min, while the growth rate for the nodule was 3.52 μm/min.
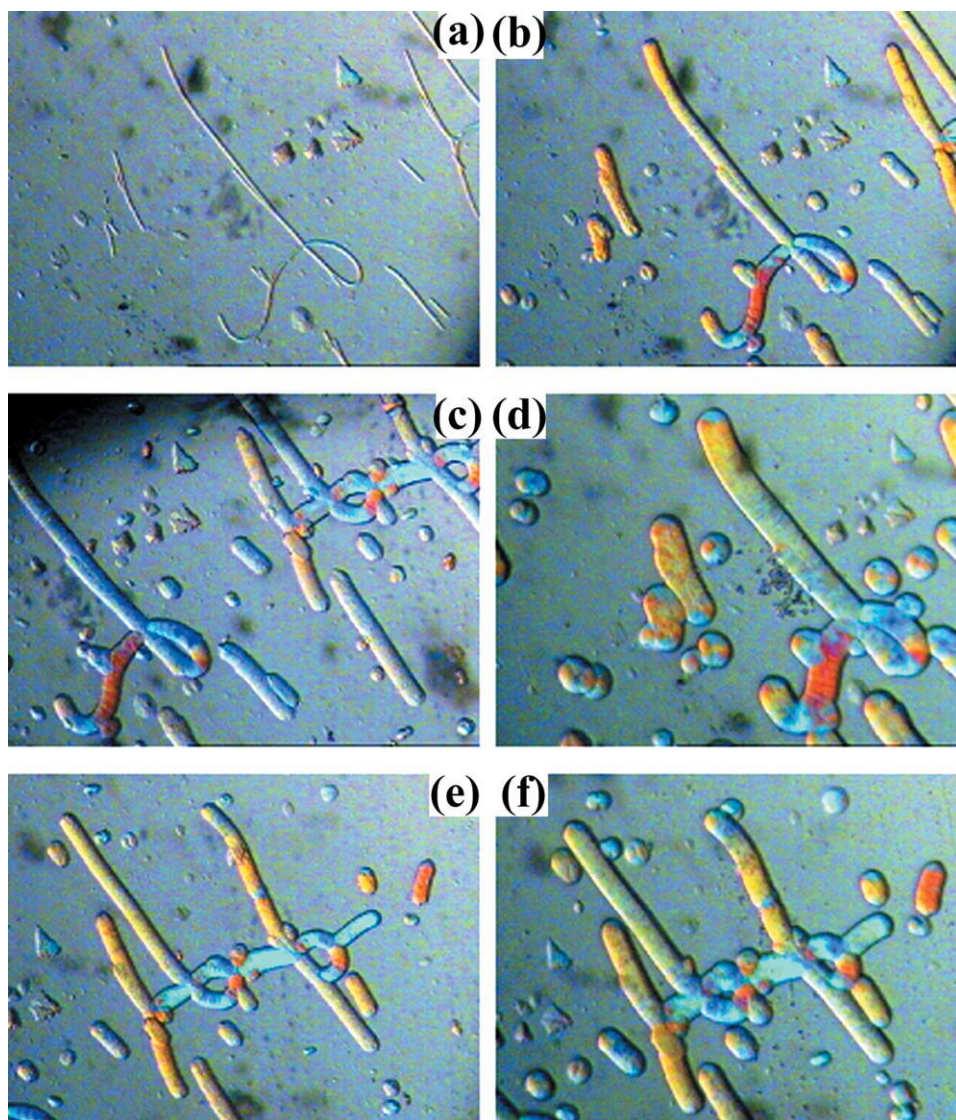
Figure 16 Images of iPP (HP525 mixed with 1 wt % nanofil 9) isothermally crystallized at 135°C. The melt temperature was 185°C (magnification = 190×). [Color figure can be viewed in the online issue, which is available at wileyonlinelibrary.com.]

Similar observation was reported by Yan et al.[27] where the crystallization behavior of partially melting iPP has been carefully examined. The authors reported that the unmelted material can accelerate the primary nucleation rate, and the ordered structure of polymer melt can speed up the linear growth rate of spherulite, and so the crystallization of partially melting iPP proceeds very quickly. It is also indicated that the crystallization mechanism of iPP ordered melt after partial melting is different from that of unperturbed equilibrium melt. In the present work, iPP samples were completely melted before the crystallization step carried out, and both individual spherulites and nodules were observed upon crystallization.

Another observation should be noted is the reproducibility of the nodular structure, which appears within the crystallized iPP as long as the sample's temperature does not exceed 190–195°C. Once iPP sample's temperature exceeds this value, nodules will never form again.

Nodular structure of different iPP resins

To check the existence of the same phenomenon with other iPP samples, another seven grades were investigated. These grades are Sabic 578P, Total M3661, Total PPH5042, FINA 4042S, Moplen HP525J mixed with 1 wt % of nanofil 9, Moplen HP525J mixed with 5 wt % PBA, and Moplen HP525J mixed with 10 wt % PBA. The series of Figures 13–19 displays the set of images for iPP samples melt crystallized isothermally at 135°C, all these samples were initially heated up to 185°C passing their melting temperature and kept for 3 min at this temperature.
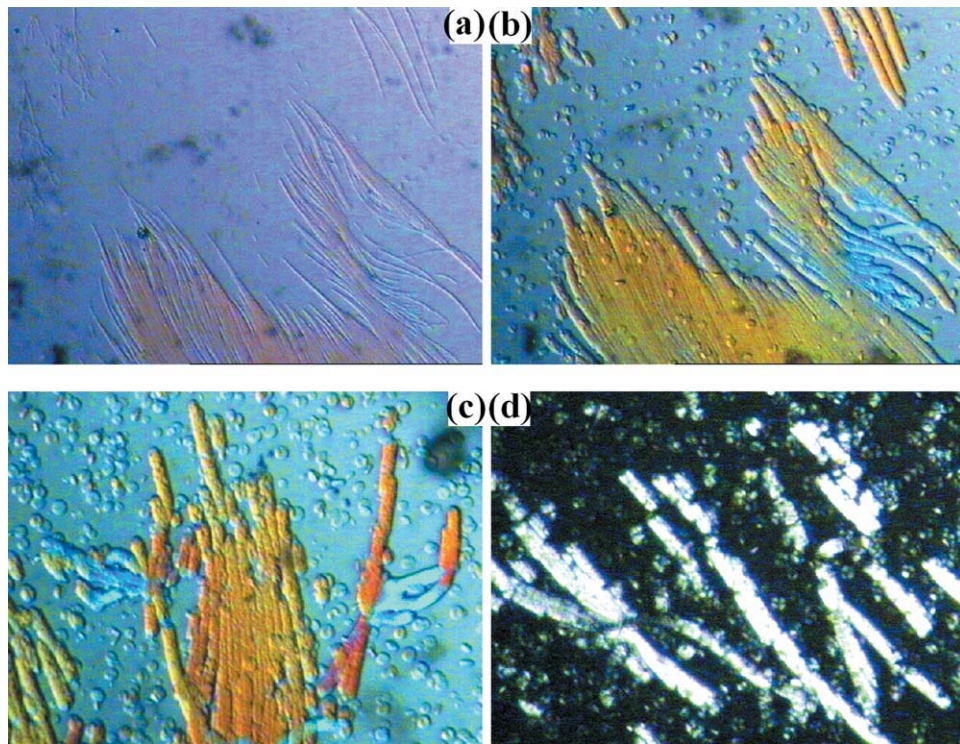
Figure 17 Images of iPP (Total PPH5042) isothermally crystallized at 135°C. The melt temperature was 185°C (magnification = 190×). [Color figure can be viewed in the online issue, which is available at wileyonlinelibrary.com.]

The same phenomenon can be observed clearly for all iPP grades used in the study where nodular structure is formed as the samples cooled from 180 to 135°C. The nodules have different shapes as clearly seen: straight shapes as shown in Figures 3, 6(a,b), 7(c,d), 14(a), 17, and 18(c), circular as shown
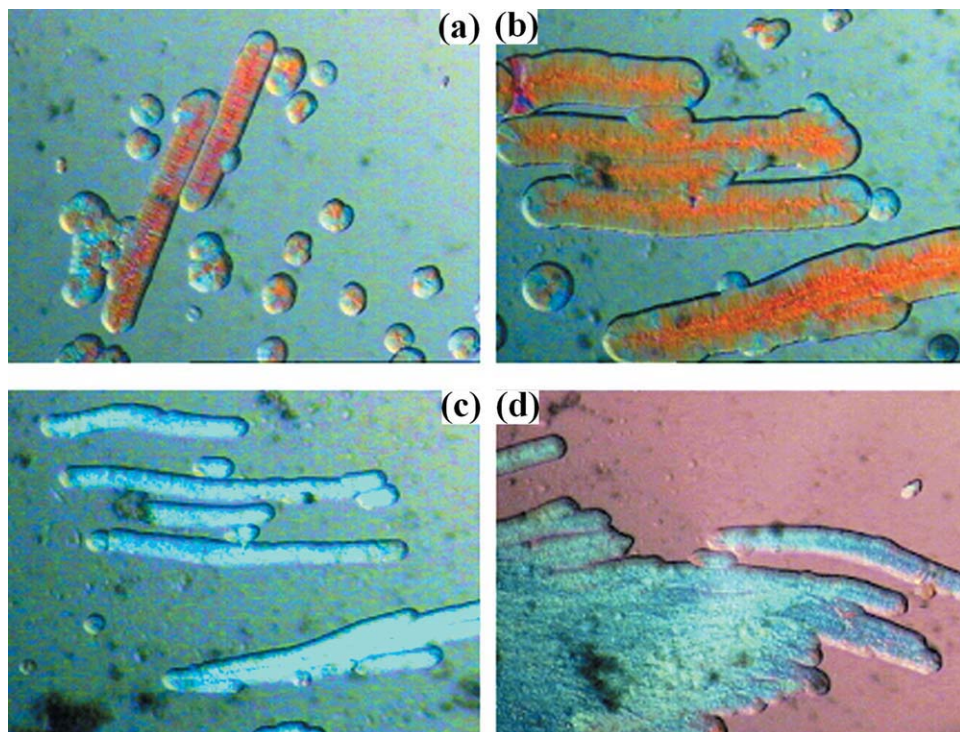

Figure 18 Images of iPP (Grade 578P) isothermally crystallized at 135°C. The melt temperature was 185°C (magnification = 190×). [Color figure can be viewed in the online issue, which is available at wileyonlinelibrary.com.]

Figure 19 Images of iPP (FINA 4042S) isothermally crystallized at 135°C. The melt temperature was 185°C (magnification = 190×). [Color figure can be viewed in the online issue, which is available at wileyonlinelibrary.com.]
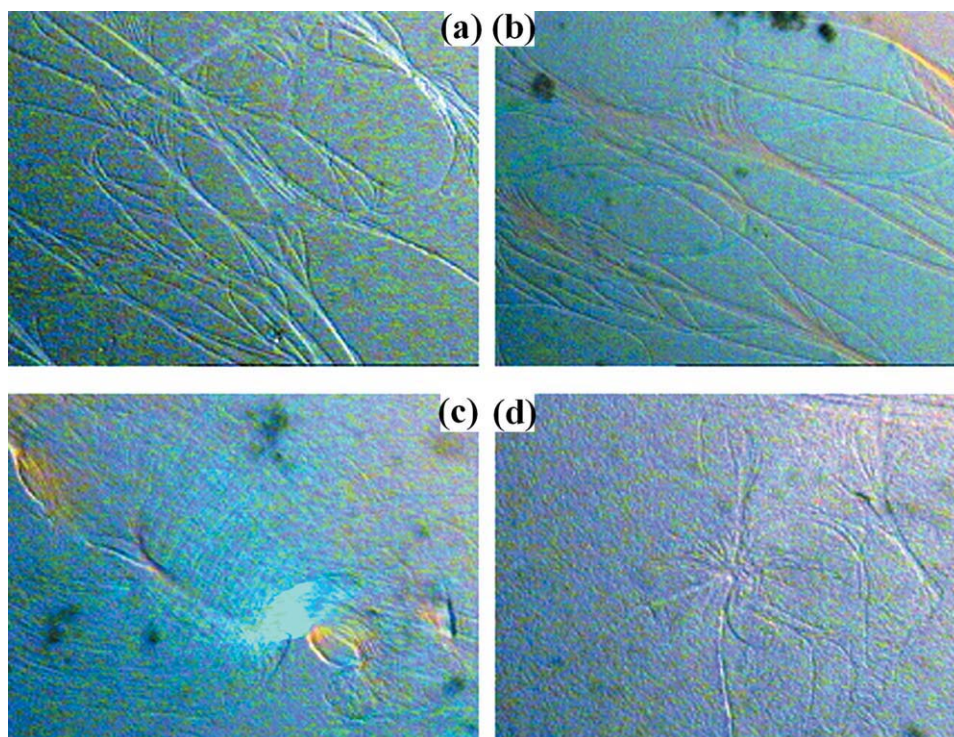
in Figures 6(c,d), 7(a,b), 13(c), and 16, entangled as shown in Figures 8, 13, 14(c,d), and 19, and branched as shown in Figures 13 and 17(c). Another observation should be mentioned about the arrangement of these nodules within the samples, and they grow in parallel directions as shown in Figures 3, 6(a,b), 7(c,d), 14(a), 15(a,b), and 18(c), crossed as shown in Figures 7(a,b), 13(a,c), and 14(d), and in a random way as shown in Figures 13(e,f), 14(b), 17(c), and 19.

Composite samples, prepared by mixing iPP (HP525J grade) with a nanofiller or BPA in a brabender and then extruded, showed similar behavior. Figures 14–16 prove that the nodular structure can be obtained not only for virgin iPP resins but also for processed iPP.

Crystallization of iPP into nodular structure could also be obtained for samples crystallized nonisothermally from the melt at different cooling rates. It is noticed that nodules were obtained for all samples nonisothermally crystallized within a cooling rate ranged from 0.5 to 20°C/min. An increase in the intensity of the nodules was observed as the cooling rate increases, increasing the cooling rate from 0.5 to 20°C/min decreases the size of nodules; the instantaneous crystallization of a large number of nodular domains restricts their lateral growth and suggests the formation of a large number of nuclei within the sample. It is also observed that the instantaneous

crystallization results in a random orientation of nodular domains, with respect to each other.

Two sets of isothermal (125, 130, 135, 140, and 145°C) and nonisothermal (0.5, 1, 2, 5, 10, and 20°C/min) crystallization experiments were carried out. A comparison between the crystallization and growth rates of both the spherulites and the nodules are under preparation and will be presented in details in another work.

CONCLUSIONS

It is concluded that for iPP, a nodular structure can be obtained not only by recrystallization from the glassy state or annealing of mesomorphic structure but also by crystallization directly from the melt.

If iPP is heated up to a temperature above its melting temperature and below 190–195°C and then cooled down to a temperature below its melting temperature it will crystallize in a nodular form. The quantity of the formed nodules depends on the temperature of the molten phase; it is found that increasing the molten phase temperature results in a reduction in the intensity of the final nodules formed within the sample.

Nodular structure can be obtained as long as the sample's temperature does not exceed 195°C. Once the temperature exceeds this value, nodules will

never form if the sample crystallizes from the melt. Nodular structure can be obtained at a wide range of melt crystallization temperatures.

The shape of the formed nodules can be straight, circular, branched, or entangled, and they can grow parallel to each other or they can be crossed or in a random way.

For spherulites and nodules grown in the same iPP sample, it is found that the linear growth rate of the spherulite and the circumferential growth rates of the nodules are very close to each other, with individual spherulite growing a little faster than the nodule.

In comparison with growth rates of individual spherulite growing in a sample heated up to 200°C and isothermally crystallized from the melt at 135°C, nodules grow faster when they crystallize in a sample heated up to 185°C and then melt crystallize at the same crystallization temperature.

References

1. Hans-Georg, E. An Introduction to Plastics. Weinheim: VCH, 1993.
2. Karger-Kocsis, J. Polypropylene Structure, Blends and Composites: Structure and Morphology, Vol. 1. London: Chapman and Hall, 1995.
3. Mezghani, K.; Phillips, P. J. Polymer 1997, 38, 5725.
4. Aboulfaraj, M.; Ulrich, B.; Dahoun, A.; G'sell, C. Polymer 1993, 34, 4817.
5. Hsu, C. C.; Geil, P. H.; Miyaji, H.; Asai, K. J Polym Sci Part B: Polym Phys 1986, 24, 2379.
6. DeSantis, F.; Adamovsky, S.; Titomanlio, G.; Schick, C. Macromolecules 2006, 39, 2562.
7. Maier, C.; Calafut, T. Polypropylene: The Definitive User's Guide and Data Book. New York: Plastics Design Library, 1998.
8. Ferrer-Balas, D.; Maspoch, M. L.; Martinez, A. B.; Santana, O. O. Polymer 2001, 42, 1697.
9. Poussin, L.; Bertin, Y. A.; Parisot, J.; Brassy, C. Polymer 1998, 39, 4261.
10. Gezovich, D. M.; Geil, P. H. Polym Eng Sci 1968, 8, 202.
11. Ogawa, T.; Miyaji, H.; Asai, K. J Phys Soc Japan 1985, 54, 3668.
12. Norton, D. R.; Keller, A. Polymer 1985, 26, 704.
13. Caldas, V.; Brown, G. R.; Nohr, R. S.; MacDonald, J. G.; Raboin, L. E. Polymer 1994, 35, 899.
14. Risnes, O. K.; Mather, R. R.; Neville, A. Polymer 2003, 44, 89.
15. Xu, T.; Lei, H.; Xie, C. S. Mater Des 2003, 24, 227.
16. Konishi, T.; Nishida, K.; Kanaya, T. Macromolecules 2006, 39, 8035.
17. Zia, Q.; Androsch, R.; Radusch, H. J.; Piccarolo, S. Polymer 2006, 47, 8163.
18. Zhao, J.; Qiu, J.; Niu, Y.; Wang, Z. J Polym Sci Part B: Polym Phys 2009, 47, 1703.
19. Sterzynski, T.; Calo, P.; Lambla, M.; Thomas, M. Polym Eng Sci 1997, 37, 1917.
20. Hsu, C. C.; Geil, P. H. J Appl Phys 1984, 56, 2404.
21. Hsu, C. C.; Geil, P. H. Polym Commun 1986, 27, 105.
22. Wunderlich, B. Macromolecular Physics, Vol. 3. New York: Academic Press, 1980.
23. Lu, H.; Qiao, J.; Xu, Y.; Yang, Y. J Appl Polym Sci 2002, 85, 333.
24. Cho, K.; Saheb, D. N.; Yang, H.; Kang, B.; Kim, J.; Lee, S. Polymer 2003, 44, 4053.
25. Mubarak, Y.; Harkin-Jones, E. M. A.; Martin, P. J.; Ahmad, M. Polymer 2001, 42, 3171.
26. Hernández-Sánchez, F.; del Castillo, L. F.; Vera-Graziano, R. J Appl Polym Sci 2004, 92, 970.
27. Zhu, X.; Li, Y.; Yan, D.; Fang, Y. Polymer 2001, 42, 9217.